

Provided for non-commercial research and education use.  
Not for reproduction, distribution or commercial use.



This article appeared in a journal published by Elsevier. The attached copy is furnished to the author for internal non-commercial research and education use, including for instruction at the authors institution and sharing with colleagues.

Other uses, including reproduction and distribution, or selling or licensing copies, or posting to personal, institutional or third party websites are prohibited.

In most cases authors are permitted to post their version of the article (e.g. in Word or Tex form) to their personal website or institutional repository. Authors requiring further information regarding Elsevier's archiving and manuscript policies are encouraged to visit:

<http://www.elsevier.com/copyright>



Contents lists available at SciVerse ScienceDirect

## European Journal of Mechanics B/Fluids

journal homepage: [www.elsevier.com/locate/ejmflu](http://www.elsevier.com/locate/ejmflu)

## Stochastic evolution equations with localized nonlinear shoaling coefficients

Yaron Toledo<sup>a,\*</sup>, Yehuda Agnon<sup>b</sup><sup>a</sup> Institute for Hydraulics and Water Resources Engineering, Technological University Darmstadt, Darmstadt, Germany<sup>b</sup> Civil and Environmental Engineering, Technion, Haifa, Israel

## ARTICLE INFO

## Article history:

Received 23 January 2011

Received in revised form

24 August 2011

Accepted 15 January 2012

Available online 24 January 2012

## Keywords:

Surface gravity waves

Nonlinear shoaling

Triad interactions

Stochastic models

## ABSTRACT

Nonlinear interactions between sea waves and the bottom are a main mechanism for energy transfer between the different wave frequencies in the near-shore region. Nevertheless, it is difficult to account for this phenomenon in stochastic wave models due to its mathematical complexity, which consists of computing either the bi-spectral evolution or non-local shoaling coefficients. Recent advances allowed the localization of the nonlinear shoaling coefficients, setting a simpler way to apply this mechanism in these models for one-dimensional interactions. This was done by taking into account only mean energy transfers between the modes while neglecting oscillatory transfers. The present work aims to improve these localized coefficients in order to make them more consistent with the dominating resonance mechanism—the class III Bragg resonance. The approximated stochastic models are tested with respect to a deterministic nonlinear mild-slope equation model, where a significant advantage of the improved coefficients is observed.

© 2012 Elsevier Masson SAS. All rights reserved.

## 1. Introduction

Nonlinear energy transfer is a dominant process that affects the evolution of wave spectra both in deep water and in the shoaling region. The nonlinear interactions in deep water consist of wave quartet interactions at leading order. These wave quartets, which act at cubic nonlinearity in wave steepness, satisfy resonant conditions of the wave frequencies and wave numbers. This type of evolution is rather a weak one that requires large spatial distances (time) of thousands of wavelengths (wave periods) in order to have a considerable effect. In intermediate to shallow water, the nonlinear interactions act much faster with significant energy transfers between triads of waves. This is possible due to the influence of the bottom that enables us to satisfy the resonant conditions already in quadratic nonlinearity. Furthermore, when waves shoal their steepness increase, and as nonlinear interactions are proportional to the wave steepness, the nonlinear energy transfer becomes even larger in this region.

Various wave models address the problem of nonlinear interactions in the near shore environment. Boussinesq-type equations reduce one spacial dimension assuming the depth is small compared to the wavelength. These equations can compute the nonlinear time-domain problem with great accuracy (see, e.g. [1]), but result in a very high computer effort. Other methods assume a set of slowly evolving harmonic wave components with a

vertical profile that fits the linear motion over a flat bottom (mild-slope-type assumptions). This approach results in a set of evolution equations for each harmonic that are coupled with quadratic nonlinear terms. These equations can be hyperbolic (e.g. [2]), elliptic and parabolic (e.g. [3–5]).

The advantage of using a stochastic approach is the significant reduction in calculation effort, as the Nyquist limitation no longer restricts the numerical solution. Several works on stochastic wave models that account for nonlinear interactions were presented. Agnon and Sheremet [6,7], Kofoed-Hansen and Rasmussen [8], Eldeberky and Madsen [9] presented stochastic evolution equations based on hyperbolic models taking into account one-dimensional interactions. Herbers and Burton [10] derived stochastic evolution equations starting from a Boussinesq-type model while presenting as well two-dimensional calculations for the quasi-one-dimensional problem (no bottom changes in the lateral direction). Janssen et al. [4] derived a stochastic model, using a Fourier transform in the lateral direction. Their model includes diffraction effects, while accounting for two-dimensional quadratic nonlinear interactions that allow mild changes in the lateral direction.

The common and most widely used forecasting models are based on a stochastic hyperbolic wave action equation. In these models, simplified one-dimensional parametric source functions are used to describe the triad interactions (see [11,12]). In these source functions there is only energy transfer to higher harmonics of each spectral component (self-interactions) without accounting for other transfers of energy of different triad combinations and energy that is transferred to lower harmonics. This approach

\* Corresponding author.

E-mail address: [aron.toledo@gmail.com](mailto:aron.toledo@gmail.com) (Y. Toledo).

enables an easy inclusion of simplified nonlinear energy transfers, but may lead to a physically inappropriate evolution of the spectrum (see [13,12]). In addition, the derivation of parametric source functions consists of a local flat bottom approximation. As oscillating bottom components, which enable satisfaction of wave number resonance conditions, come as well from the bottom profile's derivatives, it inherently fails to accurately model the dominating energy transfer—the class III Bragg resonance.

Here lies a wide gap. On one hand there are stochastic models such as [4] that take into account the directional spreading of the triad interactions, but on the other hand this physics is not applied to the wave forecasting models even for the one-dimensional case. The problem in including the two-dimensional quadratic interaction model of [4] is that it is based on a Fourier transform in the lateral direction that poses a problem in applying it to the hyperbolic formulation of the wave action equation models. Furthermore, for these forecasting models even the calculation of the one-dimensional quadratic interactions is costly for its inclusion, as these models are run in real time for very large spacial and temporal domains. Hence, a lighter quadratic nonlinear model is required in order to present an alternative approach that still grasps the essence of this important phenomenon.

Among the aforementioned stochastic works a main advancement in reducing the bi-spectral calculation costs was made by Agnon and Sheremet [6]. They presented an analytical definition of the bi-spectra that allows its substitution into the evolution equations without the need for its direct numerical calculation. Still, due to this operation the resulting interaction coefficients became non-local, and therefore, difficult to apply to forecasting models.

In a later work, Agnon and Sheremet [7] improved the accuracy of the nonlinear triad interactions. In addition, they localized the non-local coefficients by assuming the bottom to be a sum of oscillating components. More recent progress was made by Stiassnie and Drimer [14], who managed to localize the non-local shoaling coefficients of [6] by neglecting harmonic back and forth energy transfers between the modes and accounting only for the mean energy transfer. This progress paves the way for applications of this approach for one-dimensional interactions also in two-dimensional wave action equation-type forecasting models, as it significantly lowers the computational effort, while still incorporating the mean energy transfer between all wave triad combinations.

The present work aims to apply the method of Stiassnie and Drimer [14] to the more accurate one-dimensional non-local shoaling coefficients of Agnon and Sheremet [7]. This simplistic approach is not supposed to compete with more accurate models such as the ones of Herbers and Burton [10], Agnon and Sheremet [7] and Janssen et al. [4] but rather improve another line of work—the simpler localized nonlinear interaction terms appropriate for wave forecasting models given by Elderbeky and Battjes [11], Becq-Girard et al. [12] and Stiassnie and Drimer [14].

The paper is constructed as follows. In Section 2, an overview is given on resonant interactions in the near-shore region. The stochastic model of Agnon and Sheremet [7] is presented in Section 3 together with the non-local nonlinear shoaling coefficients. In Section 4 the non-local shoaling coefficients of [7] are inspected. Then, new local shoaling coefficients are derived and compared together with the coefficients of [14] to the non-local coefficients of Stiassnie and Drimer [7]. Numerical calculations are presented in Section 5, and the work is summarized in Section 6.

## 2. Resonant interactions

In order to better understand the nonlinear interactions in the shoaling region, it is helpful to observe the problem in the frequency and wavenumber domains with respect to resonant

interactions. These resonant interactions (as well as near resonant ones) represent the majority of energy transfer within the wave spectrum. For a wave field in deep water, interactions among different wave components become resonant at order  $m$  (in wave steepness), if the wavenumbers  $k_j$  and the corresponding frequencies  $\omega_j$  satisfy resonance conditions. This requires the sum of wavenumbers and frequencies to satisfy the following relations

$$\omega_1 \pm \omega_2 \pm \dots \pm \omega_{m+1} = 0, \quad \mathbf{k}_1 \pm \mathbf{k}_2 \pm \dots \pm \mathbf{k}_{m+1} = 0, \quad (1)$$

$$m \geq 1.$$

As the wave number and the frequency of each wave are related through the dispersion relation, the satisfaction of Eq. (1) in deep water can not occur at  $m = 2$  (i.e. between wave triads). Therefore, the leading order interaction is of a quadruplet of waves at  $m = 3$ , which is supplemented by weaker interactions at  $m = 4, 5, \dots$ . In shallow to intermediate waters, a bottom-induced free-surface interference, which does not abide by the dispersion relation, can allow the satisfaction of this resonance relation (1) even at order  $m = 1$ . These resonant interactions, which consists of bottom components in addition to surface wave ones, relate to the so-called Bragg resonance.

The linear class I and class II Bragg resonances occur at order  $m = 1$  with one bottom component and with two bottom components respectively. The nonlinear class III Bragg resonance occurs at order  $m = 2$  with one bottom component. The class I and class II Bragg resonances are the wavenumber representation of the main linear reflection and refraction effects, whereas the class III Bragg resonance is the main wavenumber representation of the nonlinear triad interactions in shallow to intermediate depths. Eq. (1) can be used to describe higher orders of linear and nonlinear interactions with more bottom components, but these interactions usually have a lesser effect. Different terms in wave equations can be ordered using this classification. For simplification purposes, these equations can be truncated in a consistent way above a chosen Bragg class resonance order.

For  $m = 2$  with one bottom component, Eq. (1) takes the form:

$$\omega_1 \pm \omega_2 \pm \omega_3 = \gamma, \quad \mathbf{k}_1 \pm \mathbf{k}_2 \pm \mathbf{k}_3 \pm \mathbf{K}_n = \delta. \quad (2)$$

Here,  $\mathbf{K}_n$  is a bottom component, and small detuning parameters,  $\delta$  and  $\gamma$ , have been added in order to represent the near resonant interactions. Eq. (2) describes the class III Bragg resonance conditions.

## 3. Stochastic models

In this section the development of [6,7] is presented. For the one-dimensional case Agnon and Sheremet obtained the following equation:

$$\frac{d \langle |B_f|^2 \rangle}{dx} = 2 \sum_{f_1} \sum_{f_2} \tilde{W}_{(0,1,2)} \Im m \times \left[ \langle B_f^* B_{f_1} B_{f_2} e^{-i \int_{-\infty}^x \Delta_{0;1,2} dx'} \rangle \right] \delta_{f, f_1+f_2} - 2 \sum_{f_1} \sum_{f_2} \tilde{W}_{(0,-1,2)} \Im m \times \left[ \langle B_f^* B_{f_1}^* B_{f_2} e^{-i \int_{-\infty}^x \Delta_{2;0,1} dx'} \rangle \right] \delta_{f_2, f+f_1}. \quad (3)$$

Here,

$$B_f = Cg_f^{1/2} A_f \quad (4)$$

with  $Cg_f$  as the modal group velocity from linear theory and  $A_f$  as the modal amplitude. The notation  $\langle \dots \rangle$  represents an ensemble

average;  $\Im m$  represents the imaginary part;  $\Delta_{0:1,2} = k_f - k_{f_1} - k_{f_2}$  is the triad wave number mismatch, and the kernel  $\tilde{W}$  is given by

$$\begin{aligned} \tilde{W}_{(0,\pm 1,2)} = & \frac{g}{8 (Cg_f Cg_{f_1} Cg_{f_2})^{1/2}} \\ & \times \left[ \pm (2 - \Gamma^\pm) k_{f_1} k_{f_2} + (1 - \Gamma^\pm) \frac{\omega_{f_1}^2 \omega_{f_2}^2}{g^2} \right. \\ & \left. + k_{f_1}^2 \frac{\omega_{f_2}}{\omega_f} \pm k_{f_2}^2 \frac{\omega_{f_1}}{\omega_f} \mp (1 - \Gamma^\pm) \frac{\omega_f^2 \omega_{f_1} \omega_{f_2}}{g^2} \right]. \end{aligned} \quad (5)$$

The relation between the modal frequency  $\omega_f$  and the modal wave number  $k_f$  is subject to the linear dispersion relation

$$\omega_f^2 = gk_f \tanh k_f h,$$

and Eldeberky and Madsen's [9] correction to the original kernel of [6] is given as

$$\Gamma^\pm = 2Cg_f (k_f \mp k_{f_1} - k_{f_2}) / \omega_f.$$

Note that this nonlinear correction applies for transferring the potential amplitude to the wave elevation amplitude, i.e. when  $\Gamma^\pm = 0$ ,  $A_f$  relates to the velocity potential's amplitude instead of the surface elevation's one.

In Eq. (3), the evolution of  $\langle |B_f|^2 \rangle$  in the l.h.s is related to third order nonlinear interactions in the r.h.s., which are proportional to the bi-spectra. Solving these bi-spectral interactions is time consuming. If one tries to substitute it using the evolution equation of  $B_f$ , it results in a residue containing four wave nonlinear interactions and so on. Hence, in order to solve this problem a closure relation is needed.

Agnon and Sheremet [6,7] used a closure given by the theory of weak turbulence of [15]. For leading order energy transfer, this closure condition relates four-wave nonlinear interactions to products with repeated indices, and enables construction of an evolution equation for the bi-spectra as

$$\begin{aligned} \frac{d}{dx} \langle B_f^* B_{f_1} B_{f_2} \rangle = & 2i \left[ \tilde{W}_{(0,1,2)} \langle |B_{f_1}|^2 \rangle \langle |B_{f_2}|^2 \rangle \right. \\ & + \tilde{W}_{(1,-2,0)} \langle |B_{f_2}|^2 \rangle \langle |B_f|^2 \rangle \\ & + \tilde{W}_{(2,-1,0)} \langle |B_{f_1}|^2 \rangle \langle |B_f|^2 \rangle \left. \right] \\ & \times e^{i \int_{-\infty}^x \Delta_{0:1,2} dx'} \delta_{f, f_1 + f_2}, \end{aligned} \quad (6)$$

$$\begin{aligned} \frac{d}{dx} \langle B_f^* B_{f_1}^* B_{f_2} \rangle = & -2i \left[ \tilde{W}_{(0,-1,2)} \langle |B_{f_1}|^2 \rangle \langle |B_{f_2}|^2 \rangle \right. \\ & + \tilde{W}_{(1,-0,2)} \langle |B_{f_2}|^2 \rangle \langle |B_f|^2 \rangle \\ & + \tilde{W}_{(2,1,0)} \langle |B_{f_1}|^2 \rangle \langle |B_f|^2 \rangle \left. \right] \\ & \times e^{-i \int_{-\infty}^x \Delta_{2:0,1} dx'} \delta_{f_2, f + f_1}. \end{aligned} \quad (7)$$

Eqs. (6) and (7) were solved and applied to Eq. (3) to yield a one-dimensional model for stochastic waves propagating over uneven topography:

$$\begin{aligned} \frac{d \langle |B_f|^2 \rangle}{dx} = & 4 \sum_{f_1} \sum_{f_2} \left[ \Re \left[ \mathcal{K}_{0:1,2} \right] \langle |B_{f_1}|^2 \rangle \langle |B_{f_2}|^2 \rangle \right. \\ & + \Re \left[ \mathcal{K}_{1:-2,0} \right] \langle |B_{f_1}|^2 \rangle \langle |B_f|^2 \rangle \\ & + \Re \left[ \mathcal{K}_{2:-1,0} \right] \langle |B_{f_2}|^2 \rangle \langle |B_f|^2 \rangle \left. \right] \\ & \times \tilde{W}_{(0,1,2)} \delta_{f, f_1 + f_2} \end{aligned}$$

$$\begin{aligned} & + 8 \sum_{f_1} \sum_{f_2} \left[ \Re \left[ \mathcal{K}_{0:-1,2} \right] \langle |B_{f_1}|^2 \rangle \langle |B_{f_2}|^2 \rangle \right. \\ & + \Re \left[ \mathcal{K}_{1:-0,2} \right] \langle |B_{f_2}|^2 \rangle \langle |B_f|^2 \rangle \\ & + \Re \left[ \mathcal{K}_{2:1,0} \right] \langle |B_{f_1}|^2 \rangle \langle |B_f|^2 \rangle \left. \right] \\ & \times \tilde{W}_{(2,1,0)} \delta_{f_2, f + f_1}, \end{aligned} \quad (8)$$

where the shoaling interaction function  $\mathcal{K}$  appearing in Eq. (8) is defined as

$$\mathcal{K}_{0:1,2} = e^{-i \int_{-\infty}^x \Delta_{0:1,2} dx'} \int_{-\infty}^x \tilde{W}_{(0,1,2)} e^{i \int_{-\infty}^x \Delta_{0:1,2} dx'} dx'. \quad (9)$$

In the work of Agnon and Sheremet [6] the kernel  $\tilde{W}$  was assumed to be varying slowly, and Eq. (9) was approximated as

$$\mathcal{K}_{0:1,2} = \tilde{W}_{(0,1,2)} \mathcal{J}_{0:1,2}, \quad (10)$$

$$\mathcal{J}_{0:1,2} = e^{-i \int_{-\infty}^x \Delta_{0:1,2} dx'} \int_{-\infty}^x e^{i \int_{-\infty}^x \Delta_{0:1,2} dx'} dx'. \quad (11)$$

As can be seen in Eqs. (9) and (11) the shoaling coefficients are non-local (i.e. containing spatial integrations). These coefficients are difficult to apply in two-dimensional models. In this case, the bi-spectrum is not evolving along a straight line in the manner that was presented in Eqs. (6) and (7), but rather as a two-dimensional field, where the wave ray paths are unknown a priori. This prevents us from using this non-local approach. Nevertheless, these coefficients consist of local effects in addition to the non-local ones. These local parts pose no difficulty in their application to two-dimensional forecasting models. This should allow construction of an approximated one-dimensional nonlinear triad interaction source term for waves that are propagating in the same direction also for a two-dimensional wave field.

#### 4. The local shoaling coefficients

Let us inspect the non-local shoaling coefficient  $\mathcal{K}$ . A differential equation definition equivalent to the integral one of Eq. (9) can be written as

$$\frac{d \mathcal{K}_{0:1,2}}{dx} + i \Delta_{0:1,2} \mathcal{K}_{0:1,2} = \tilde{W}_{(0,1,2)}. \quad (12)$$

When the wave numbers are constant as in the case of deep water or a flat bottom, an analytical solution can be given. This solution consists of a homogeneous part and a particular part as follows

$$\mathcal{K}_{0:1,2} = e^{-i \Delta_{0:1,2} x} + \tilde{W}_{(0,1,2)} \left( \pi \delta(\Delta_{0:1,2}) - \frac{i}{\Delta_{0:1,2}} \right). \quad (13)$$

The wavenumber components of the wavenumber mismatch  $\Delta$  are subject to the dispersion relation and their corresponding frequencies close to zero. Therefore, the wavenumber mismatch is always nonzero, and the particular solution is purely an imaginary number. As only the real part of  $\mathcal{K}$  is taken into account in Eq. (8), the contribution in this case is solely of the homogeneous part, which is an oscillating function. This shows that in deep water or over a flat bottom, energy transfers back and forth between the modes in a harmonic manner, and no mean energy transfer is present.

In the near-shore region, variations of the kernel  $\tilde{W}$  due to changes in the bottom depth result in a nonzero real part of the particular solution, which signifies a mean transfer of energy. This can be seen as well in the wave number domain, where  $\tilde{W}$  is written as a sum of oscillating components. Several components of this sum satisfy the resonance (and near resonance) conditions

(2), and cause a significant energy transfer between the modes on top of energy that is shifting continuously back and forth. The same logic applies to derivatives of  $\tilde{W}$  as they also yield components that satisfy the resonance condition. This implies that the approximation given in Eqs. (10) and (11) is unjustified.

In order to account for the additional contribution of the derivatives of  $\tilde{W}$ , let us apply the method of Stiassnie and Drimer [14] for localizing the shoaling coefficient given in Eq. (9) without the approximation (10). The first step is to change the integration variable of Eq. (9) yielding

$$\mathcal{K}_{0:1,2} = e^{-i\zeta(x)} \int_0^{\zeta(x)} \frac{\tilde{W}_{(0,1,2)}}{\Delta_{0:1,2}} e^{i\zeta'} d\zeta', \quad (14)$$

where

$$\zeta(x) = \int_{-\infty}^x \Delta_{0:1,2} dx', \quad dx = \Delta_{0:1,2} d\zeta. \quad (15)$$

Then, by applying integration by parts, Eq. (14) takes the form

$$\begin{aligned} \mathcal{K}_{0:1,2} = & -e^{-i\zeta(x)} \left[ \frac{i\tilde{W}_{(0,1,2)}}{\Delta_{0:1,2}} e^{i\zeta'} \right]_0^{\zeta(x)} \\ & + ie^{-i\zeta} \int_0^{\zeta(x)} \frac{d}{d\zeta'} \left( \frac{\tilde{W}_{(0,1,2)}}{\Delta_{0:1,2}} \right) e^{i\zeta'} d\zeta'. \end{aligned} \quad (16)$$

The same procedure can be applied again to the integral in Eq. (16) to yield

$$\begin{aligned} \mathcal{K}_{0:1,2} = & e^{-i\zeta} \left[ \left( -\frac{i\tilde{W}_{(0,1,2)}}{\Delta_{0:1,2}} + \frac{d}{d\zeta'} \left( \frac{\tilde{W}_{(0,1,2)}}{\Delta_{0:1,2}} \right) \right) e^{i\zeta'} \right]_0^{\zeta} \\ & - e^{-i\zeta} \int_0^{\zeta} \frac{d^2}{d\zeta'^2} \left( \frac{\tilde{W}_{(0,1,2)}}{\Delta_{0:1,2}} \right) e^{i\zeta'} d\zeta', \end{aligned} \quad (17)$$

and so on. This actually follows the same approach that is used for deriving the Taylor series. The resulting non-local shoaling coefficient is

$$\begin{aligned} \Re e [\mathcal{K}_{0:1,2}] = & \frac{d}{d\zeta} \left( \frac{\tilde{W}_{(0,1,2)}}{\Delta_{0:1,2}} \right) - \frac{d^3}{d\zeta^3} \left( \frac{\tilde{W}_{(0,1,2)}}{\Delta_{0:1,2}} \right) + \dots \\ & + (-1)^{l-1} \frac{d^{2l-1}}{d\zeta^{2l-1}} \left( \frac{\tilde{W}_{(0,1,2)}}{\Delta_{0:1,2}} \right) \\ & + \Re e \left\{ e^{-i\zeta} \left[ -\frac{i\tilde{W}_{(0,1,2)}}{\Delta_{0:1,2}} + \dots \right]_{\zeta=0} \right. \\ & \left. + i^{2l} e^{-i\zeta} \int_0^{\zeta} \frac{d^{2l}}{d\zeta'^{2l}} \left( \frac{\tilde{W}_{(0,1,2)}}{\Delta_{0:1,2}} \right) e^{i\zeta'} d\zeta' \right\}. \end{aligned} \quad (18)$$

Let us inspect the last term in Eq. (18). It consists of an oscillating term and a residual term of the above process. The oscillating part, which relates to the homogeneous solution of Eq. (12), should result in a transfer of energy back and forth between the different wave harmonics. As we are interested in local coefficients that account for mean energy transfer, this term can be neglected. The residual term is a combination of an oscillating term and higher order derivatives of  $\tilde{W}/\Delta$  that continue the series, which approximates the particular solution, for orders higher than  $l$  up to infinity. These terms consist of high-order derivatives of the bottom profile and multiplications of lower-order ones, which relate to high-order nonlinear Bragg resonance terms (such as ones containing two or more bottom components in Eq. (1)).

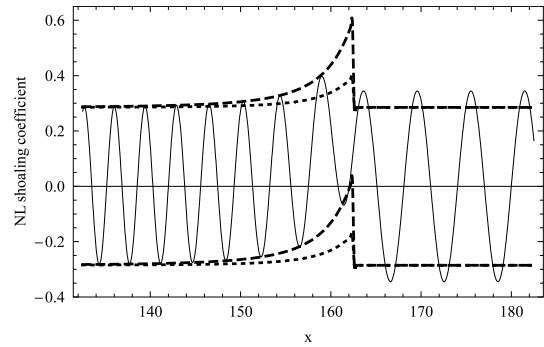


**Fig. 1.** A comparison between the nonlinear shoaling coefficients of  $\Re e [\mathcal{K}_{0:1,2}]$ : the non-local coefficient as given in Eq. (9) (solid); the local coefficient of the present work as given in Eq. (19) (dashed), and the local coefficient of [14] as given in Eq. (20) (dotted). The local coefficients were shifted up and down in the value of the non-local coefficient's amplitude in deep water. This was done in order to better present how well the local coefficients approximate the evolution of the non-local coefficient's envelope. Here, the wave triad conditions are  $f = 2\omega, f_1 = f_2 = \omega, \omega = 2\pi/T$  and  $T = 2$  s over a sloping beach of 1/25 ending with a plateau.

Neglecting these higher order Bragg resonance interactions while applying mild-slope assumptions (i.e. setting  $l = 1$ ) allows writing the nonlinear shoaling coefficients (18) as local ones, which correspond to an approximation to the particular solution of Eq. (12). After applying the chain rule, which results from Eq. (15), the shoaling coefficient takes the form

$$\Re e [\mathcal{K}_{0:1,2}] = \frac{1}{\Delta_{0:1,2}^2} \frac{d\tilde{W}_{(0,1,2)}}{dx} - \frac{\tilde{W}_{(0,1,2)}}{\Delta_{0:1,2}^3} \frac{d\Delta_{0:1,2}}{dx}. \quad (19)$$

Eq. (19) is a localized nonlinear shoaling coefficient. The same technique can be applied to all the other shoaling coefficients required for the solution of Eq. (8).

The result of [14] can be easily reproduced by following the assumptions given in Eqs. (10) and (11), i.e.  $\tilde{W}_{(0,1,2)}$  can be taken as a constant in this approximation. In this case, the local nonlinear shoaling coefficient (19) collapses to the one of [14]:

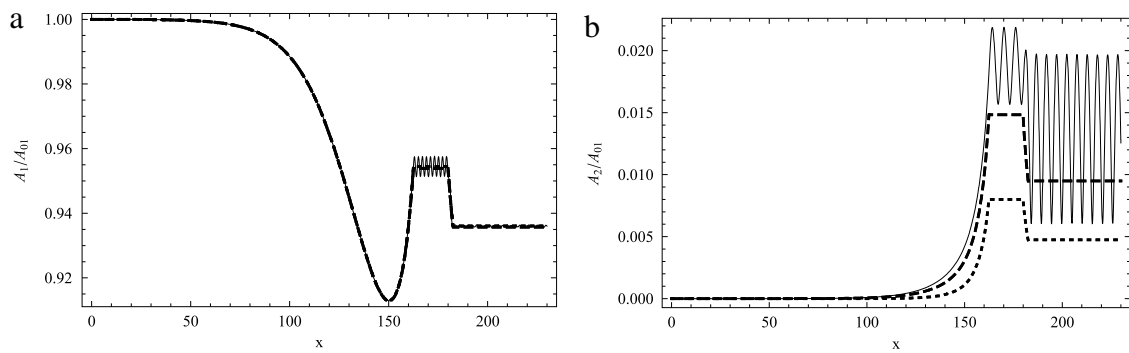
$$\Re e [\mathcal{K}_{0:1,2}] = -\frac{\tilde{W}_{(0,1,2)}}{\Delta_{0:1,2}^3} \frac{d\Delta_{0:1,2}}{dx}. \quad (20)$$

Fig. 1 presents the approximations that were made in this section by localizing the non-local nonlinear shoaling coefficient  $\Re e [\mathcal{K}_{0:1,2}]$ . The wave triad conditions are  $f = 2\omega, f_1 = f_2 = \omega, \omega = 2\pi/T$  and  $T = 2$  s over a sloping beach of 1/25 ending with a plateau. The non-dimensional water depths in the deep water start point and the shallow plateau are given as  $k_1h = 7.04, k_2h = 28.17$ , and  $k_1h = 0.77, k_2h = 2.08$  respectively. It can be seen that the new coefficient given in Eq. (19) represents the non-local coefficient's envelope evolution much better than the local coefficient of [14].

## 5. Numerical results

In order to support the use of the localized coefficient given in Eq. (19), numerical simulations will be presented in this section. These simulations will inspect the super-harmonic resonance. The results of the stochastic (phase-averaged) model (8) with the localized coefficients (19) and (20) will be compared to the ones of a deterministic nonlinear mild-slope equation model (NLMSE) of Kaihatu and Kirby [3, Eq. (22)]. As the input of the following simulations is a monochromatic wave, there is no need for a Monte Carlo type calculation, and the results can be compared as is.

In this case of a monochromatic input, the second harmonic is excited as a self-interaction of the first harmonic, and the



**Fig. 2.** The localized nonlinear stochastic models: (dashed) present work, (dotted) [14], and the deterministic nonlinear MSE (solid), for the case of a monochromatic wave of  $T = 2$  s and  $k_1 a = 0.02$  shoaling on a sloping bottom ending with a ridge with slopes of  $1/25$ . (a) First harmonic, (b) second harmonic.

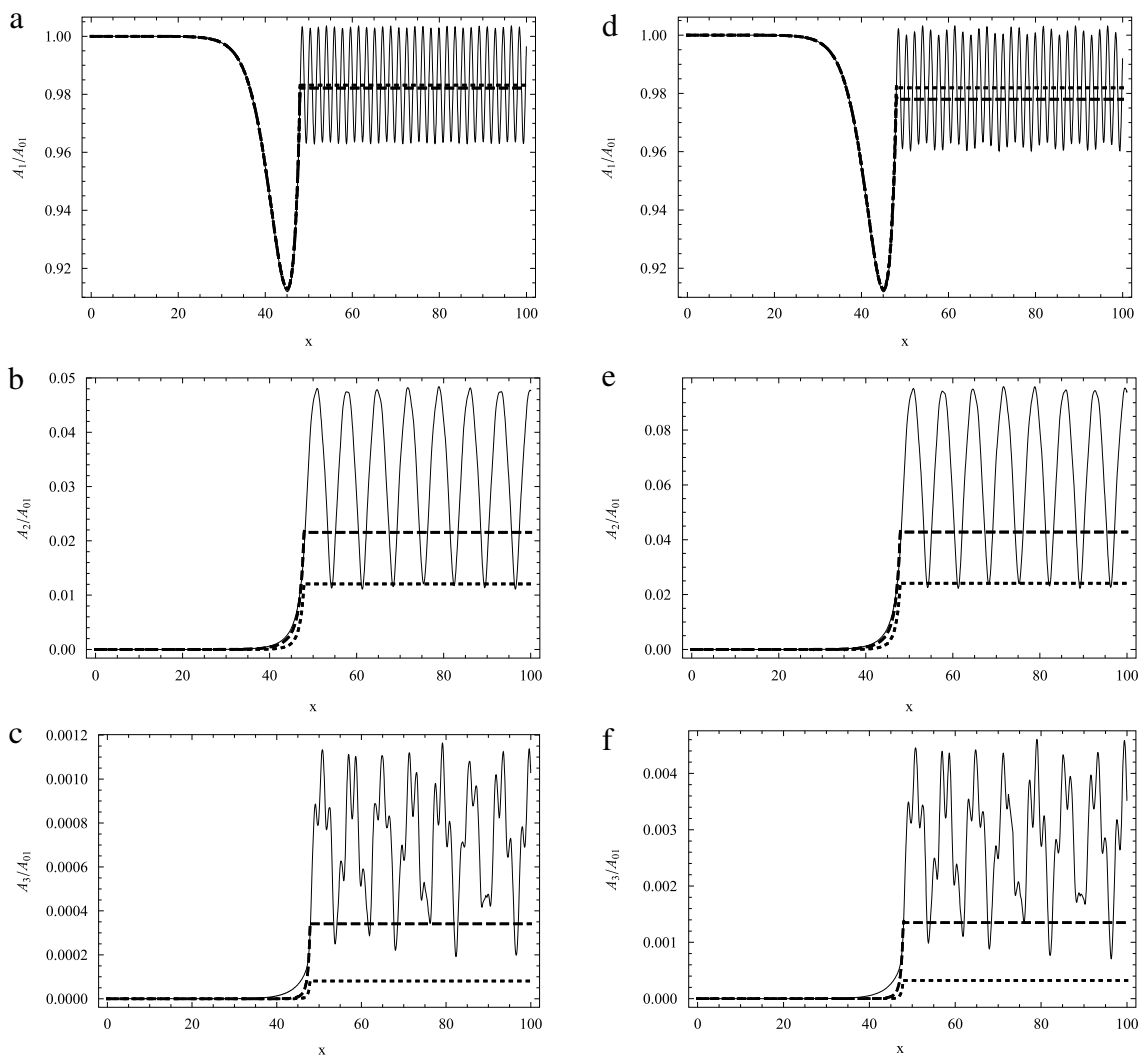


**Fig. 3.** The localized nonlinear stochastic models: (dashed) present work, (dotted) [14], and the deterministic nonlinear MSE (solid), for the case of a monochromatic wave of  $T = 2$  s and two wave steepnesses ((a–c):  $k_1 a = 0.02$ , (d–f):  $k_1 a = 0.04$ ) shoaling on a  $1/5$  sloping bottom ending with a plateau. (a, d) First harmonic, (b, e) second harmonic, (c, f) third harmonic.

third harmonic is excited by the first and second harmonics. Note that the evolution model is accurate up to quadratic order, hence the third harmonic should be underestimated due to the neglect of the cubic self-interaction of the first harmonic waves. Nevertheless, the results of quadratic nonlinear models

for the third harmonic self-interactions are still plausible (see [3,5]).

In this section, the numerical integration is done by using the Mathematica 6 software, and the amplitudes are compared as the amplitude of the velocity potential, i.e. using  $\Gamma^\pm = 0$ .

### 5.1. Waves approaching a mild sloping beach ending with a ridge

The first numerical simulation is of waves propagating on a sloped beach that ends with a ridge. The bottom profile for this case is given by

$$h(x) = \begin{cases} 7 \text{ m} - x/25 & x \leq 162.5 \text{ m} \\ 0.5 \text{ m} & 162.5 \text{ m} < x \leq 180 \text{ m} \\ 0.5 \text{ m} + x/25 & 180 \text{ m} < x \leq 182.5 \text{ m} \\ 0.6 \text{ m} & x > 182.5 \text{ m}. \end{cases} \quad (21)$$

The incident wave is a monochromatic wave with a period of  $T = 2$  s, and deep water steepness of  $k_1 a = 0.02$ . The non-dimensional depths of the two harmonics are given as  $k_1 h_{\text{deep}} = 7.04$ ,  $k_2 h_{\text{deep}} = 28.17$ ,  $k_1 h_{\text{bar}} = 0.77$ ,  $k_2 h_{\text{bar}} = 2.08$ ,  $k_1 h_{\text{shallow}} = 0.86$  and  $k_2 h_{\text{shallow}} = 2.05$ .

Results of the model of Agnon and Sheremet [7] with the two localized shoaling coefficients, i.e. Eq. (8) with either Eq. (20) or Eq. (19), are presented in Fig. 2. The results are normalized to the deep water first harmonic amplitude  $A_{01}$  and compared to the NLMSE. It can be clearly seen that the new localized nonlinear shoaling coefficient performs much better comparing to the one of [14] in the prediction of the second harmonic evolution.

### 5.2. Wave approaching a sloping beach

The second numerical simulation is of waves propagating on a steeper sloped beach that ends with a plateau. The bottom profile for this case is given by

$$h(x) = \begin{cases} 10 \text{ m} - x/5 & x \leq 48 \text{ m} \\ 0.4 \text{ m} & x > 48 \text{ m}. \end{cases} \quad (22)$$

The incident wave is a monochromatic wave with period of  $T = 2$  s. Two deep water wave steepnesses of  $k_1 a = 0.02$  and  $k_1 a = 0.04$  were investigated. The non-dimensional depths of the two harmonics are given as  $k_1 h_{\text{deep}} = 10.06$ ,  $k_2 h_{\text{deep}} = 40.24$ ,  $k_1 h_{\text{shallow}} = 0.68$ , and  $k_2 h_{\text{shallow}} = 1.72$ .

Results of the model of Agnon and Sheremet [7] with the two localized shoaling coefficients are presented in Fig. 3. As in Section 5.1, the normalized amplitudes are compared to the NLMSE. It can be seen that the new localized nonlinear shoaling coefficients perform much better than the ones of [14] in the prediction of the second and third harmonic evolution. Note that parametric models describe only wave self-interactions. Therefore, they do not yield any energy transfer to the third harmonic. This is a clear advantage of the above localized models.

## 6. Summary and conclusions

Improved one-dimensional localized nonlinear shoaling coefficients were derived for nonlinear stochastic models. These coefficients were used for the calculation of super-harmonic nonlinear energy transfer of monochromatic shoaling waves both for

steep and shallow bottom slopes. The results were in fairly good agreements with a more accurate deterministic numerical model (NLMSE).

The present derivation showed better analytical accuracy in grasping the mean behavior of the non-local coefficients. In addition, it showed significant improvement in numerical calculations of the second and third harmonics generated from a monochromatic wave-bottom quadratic nonlinear interaction for slopes of 1/25 and 1/5. The second harmonic was improved from an accuracy of 40%–43% using the model of Stiassnie and Drimer [14] to 73%–83% using the present model comparing to the NLMSE. For the third harmonic, the improvement was from ~15% to ~58%. Hence, for super-harmonic resonances of this type the general improvement was between 33% and 43% with negligible computer effort. These results support the application of these approximated coefficients as nonlinear triad interaction source terms in stochastic wave models for practical problems in order to account for one-dimensional triad interactions.

## Acknowledgments

YT is grateful for the generous support of the Max Planck Institute's Minerva postdoctoral fellowship and the German–Israel BMBF-MOST Young Scientists Exchange Program.

## References

- [1] P.A. Madsen, D.R. Fuhrman, B. Wang, A Boussinesq-type method for fully nonlinear waves interacting with a rapidly varying bathymetry, *Coastal Eng.* 53 (2006) 487–504.
- [2] Y. Agnon, A. Sheremet, J. Gonsalves, M. Stiassnie, A unidirectional model for shoaling gravity waves, *Coastal Eng.* 20 (1993) 29–58.
- [3] J.M. Kaihatu, J.T. Kirby, Nonlinear transformation of waves in finite water depth, *Phys. Fluids* 8 (1995) 175–188.
- [4] T.T. Janssen, T.H.C. Herbers, J.A. Battjes, Evolution of ocean wave statistics in shallow water: refraction and diffraction over seafloor topography, *J. Geophys. Res.* 113 (2008) C03024.
- [5] Y. Toledo, Y. Agnon, Nonlinear refraction-diffraction of water waves: the complementary mild-slope equations, *J. Fluid Mech.* 641 (2009) 509–520.
- [6] Y. Agnon, A. Sheremet, Stochastic nonlinear shoaling of directional spectra, *J. Fluid Mech.* 345 (1997) 79–99.
- [7] Y. Agnon, A. Sheremet, Stochastic evolution models for nonlinear gravity waves over uneven topography, in: Philip L.-F. Liu (Ed.), in: *Advances in Coastal and Ocean Engineering*, vol. 6, 2000, pp. 103–133.
- [8] H. Kofoed-Hansen, J.H. Rasmussen, Modeling of nonlinear shoaling based on stochastic evolution equations, *Coastal Eng.* 33 (1998) 203–232.
- [9] Y. Eldeberky, P.A. Madsen, Deterministic and stochastic evolution equations for fully dispersive and weakly nonlinear waves, *Coastal Eng.* 38 (1999) 1–24.
- [10] T.H.C. Herbers, M.C. Burton, Nonlinear shoaling of directionally spread waves on a beach, *J. Geophys. Res.* 102 (1997) 21101–21114.
- [11] Y. Elderbeky, J.A. Battjes, Parametrization of triad interaction in wave energy models, in: *Proc. Coastal Dynamics Conf.*, Gdansk, Poland, 1995, pp. 140–148.
- [12] F. Becq-Girard, P. Forget, M. Benoit, Non-linear propagation of unidirectional wave fields over varying topography, *Coastal Eng.* 38 (1999) 91–113.
- [13] M.W. Dingemans, A review of the physical formulation in SWAN, Tech. Rep. H3306, Delft Hydraulics, 1998.
- [14] M. Stiassnie, N. Drimer, Prediction of long forcing waves for harbor agitation studies, *J. Waterway Port Coastal Ocean Eng.* 132 (3) (2006) 166–171.
- [15] D.J. Benney, P.G. Saffman, Nonlinear interactions of random waves, *Proc. R. Soc. Lond. A* 289 (1966) 301–321.